THE PETAWATT LASER SYSTEM

D. M. Pennington *J. A. Britten* *J. L. Miller*
M. D. Perry *C. G. Brown* *G. Tietbohl*
B. C. Stuart *S. Herman* *V. Yanovsky*

Introduction

In this article, we describe the Petawatt laser system as it has developed into FY 1997. In May of 1996, we demonstrated the production of over a petawatt (quadrillion watts) of peak power in the Nova/Petawatt Laser Facility, generating >600 J in ~430 fs. The development of small-scale multiterawatt and now petawatt lasers has opened an entirely new regime of laser–matter interaction to exploration.[1] Applications of these extremely powerful lasers range from enabling new accelerator concepts[2] to new approaches to inertial confinement fusion (ICF).[3]

The Petawatt Laser Project was proposed in a Laboratory Directed Research and Development (LDRD) program in 1992 to develop a laser capable of producing petawatt pulses in order to examine the "fast ignitor" concept for inertial confinement fusion. Shown schematically in Figure 1, fast ignition requires high pulse energy in addition to the short pulse duration. Conventional ICF relies on creating a hot, uniformly dense central core formed by compression of a deuterium/tritium plasma. The necessity of forming the hot central core requires substantial energy and places severe requirements on implosion symmetry.[4] In the fast ignitor concept, ignition is decoupled from compression. The pellet is assembled cold and, at the point of maximum compression, is ignited by raising a small section of the pellet on the periphery of the dense core rapidly above the ignition temperature. Hot electrons (200 keV < E < 1 MeV) are generated by the interaction of the intense (10^{19}–10^{21} W/cm^2) light with plasma. The hot electrons rapidly equilibrate in the dense fuel, raising the overall ion temperature to 5 to 20 keV, which initiates fusion burn. The fusion burn then propagates throughout the compressed fuel

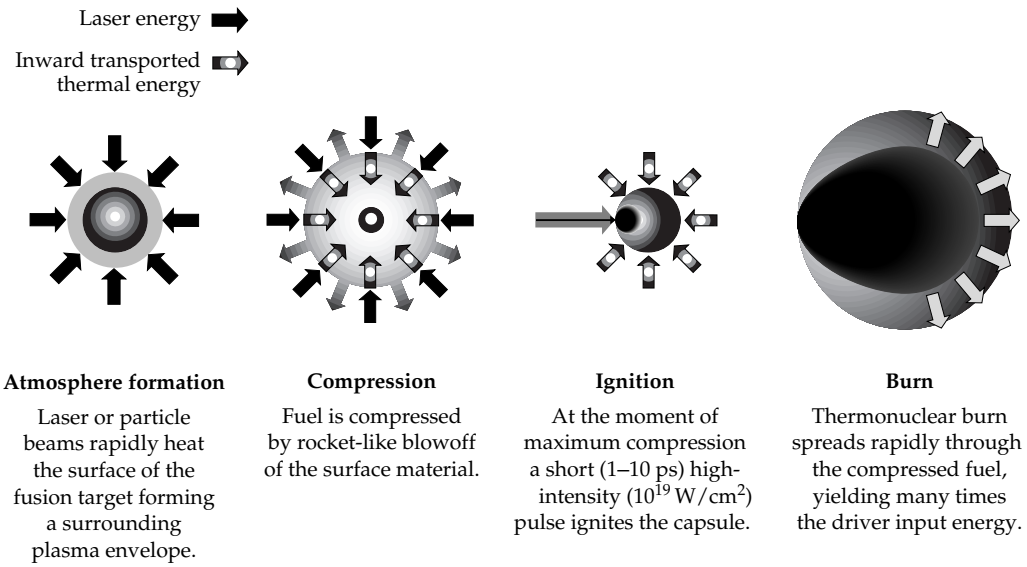

FIGURE 1. Diagram of "fast ignitor" concept in inertial confinement fusion. (70-00-0298-0179pb01)

before the hydrodynamic disassembly time of the pellet. In order to transfer enough energy to the ions in a small, well-defined volume faster than hydrodynamic disassembly, the energy must be deposited directly in the dense fuel, in a volume less than ~4000 μm^2 and a duration $\tau \leq 10$ ps, dependent on the density, convergence ratio, etc.,

$$\left(\tau \approx \frac{R_{spot}}{v_s} \leq 10 \text{ ps} \right) .$$

High laser pulse energy is required in order to produce enough hot electrons to heat the plasma sufficiently to initiate a self-sustaining fusion burn. In addition, nearly perfect beam quality is required in the laser in order to achieve a small spark region. The fast ignitor concept offers the possibility of high target gain at substantially reduced total drive energy than conventional ICF. However, unlike conventional ICF, this approach relies on untested physics in a completely new regime of laser–matter interaction.

In addition to testing the concept of fast ignition, the extreme conditions produced by the Petawatt open a new regime of laser–matter interactions to study. The short pulse duration, coupled with the enormous light pressure (>300 Gbar) and high irradiance, makes possible the production of extremely dense matter at kilovolt to megavolt temperatures. Focused irradiance above 10^{20} W/cm^2 is required to achieve the simultaneous conditions of hot (>1 keV), dense (~10^{24} cm^{-3}) matter of relevance to equation of state and hydrodynamic measurements. With an irradiance >10^{21} W/cm^2, the absorption physics enter a new regime where it may be possible to achieve high temperatures at solid density. The Petawatt will also enable the production of copious amounts of hard (10 keV to >10 MeV) x rays, which can serve as a high-energy backlighter for Nova or NIF implosions, as well as other radiographic applications.

To meet the conditions necessary to address the numerous issues associated with the fast ignitor *and* serve as a general facility for experiments in intense laser–matter interaction, the Petawatt laser was designed to produce 1-kJ pulses with a pulse duration adjustable between 0.5 and 20 ps and sufficient beam quality to produce an irradiance greater than 10^{21} W/cm^2 when focused at $f/3$.

Several new advances in technology enabled the production of petawatt pulses. One was the development of broadband laser materials for solid-state laser systems, such as Ti:sapphire. Another was the application of the chirped-pulse amplification (CPA) technique to solid-state lasers.[5-7] By stretching the pulse prior to amplification, the limitation on pulse energy imposed by beam filamentation due to small-scale self-focusing can be overcome. The CPA technique has been applied to existing, large-scale Nd:glass laser systems at CEA, Limeil,[8,9] the Rutherford-Appleton Laboratory,[10] ILE Osaka,[11] and at LLNL.[12,13]

Manufacture of pulse compression gratings of sufficient size and quality to permit the demonstration of a petawatt-scale laser was considered to be one of the most challenging tasks of the Petawatt Laser Project. To address this issue, a facility was built at LLNL, and unique processing techniques were developed to enable the fabrication of high-efficiency diffraction gratings with high laser-damage thresholds and a uniform submicron period over a length scale approaching 1 meter.[14] The final Petawatt laser design utilizes a hybrid Ti:sapphire/Nd:glass laser system in order to provide sufficient bandwidth to achieve the shortest pulse duration, large-scale diffraction gratings to compress the pulse after amplification, and compression in vacuum to avoid beam distortion and self-phase modulation resulting from the nonlinear refraction of air.

Laser System

The Petawatt laser begins with a commercial Kerr-lens mode-locked Ti:sapphire oscillator that produces transform-limited 100-fs, 1054-nm pulses. A single pulse is selected from the mode-locked train and stretched to 3 ns in a single-grating, single-lens pulse stretcher. This pulse is amplified to 6 to 7 mJ in a linear, TEM_{00}, Ti:sapphire regenerative amplifier operating at 1054 nm.[15] Further amplification to 50 mJ is achieved in a Ti:sapphire ring regenerative amplifier with a larger mode size to prevent the onset of nonlinear effects, such as self-phase modulation (SPM) and self-focusing. Up to this point, the system runs at 10 Hz with an energy stability of 3%. A pulse slicer eliminates pulse leakage from the regenerative amplifier, while a half-wave slicer switches a single pulse from the 10-Hz pulse train into the Nd:glass amplifier stage of the system. The remaining pulses are compressed to 320 fs in air for use in subterawatt level experiments[16,17] and Nova x-ray diagnostic characterization.

The pulse selected for further amplification is spatially tailored to give a near-uniform top-hat spatial profile for efficient energy extraction in mixed phosphate glass rod amplifiers, producing a spectrally shaped pulse up to 12 J in energy.[12] The beam can be propagated either to the 100-TW laser system in the Nova two-beam chamber[13] or through an image-relayed beamline, which injects the beam into Nova beamline 6 for further amplification. A 37-actuator deformable mirror will be installed in the beam at the output of the 45-mm amplifier in the master oscillator room (MOR) to precorrect for pump-induced and thermal aberrations in the Nova disk-amplifier section.

The component schematic for the Petawatt laser system is shown in Figure 2. The Nova preamplifier system has multiple stages of amplification and magnification. These optics represent a significant source of

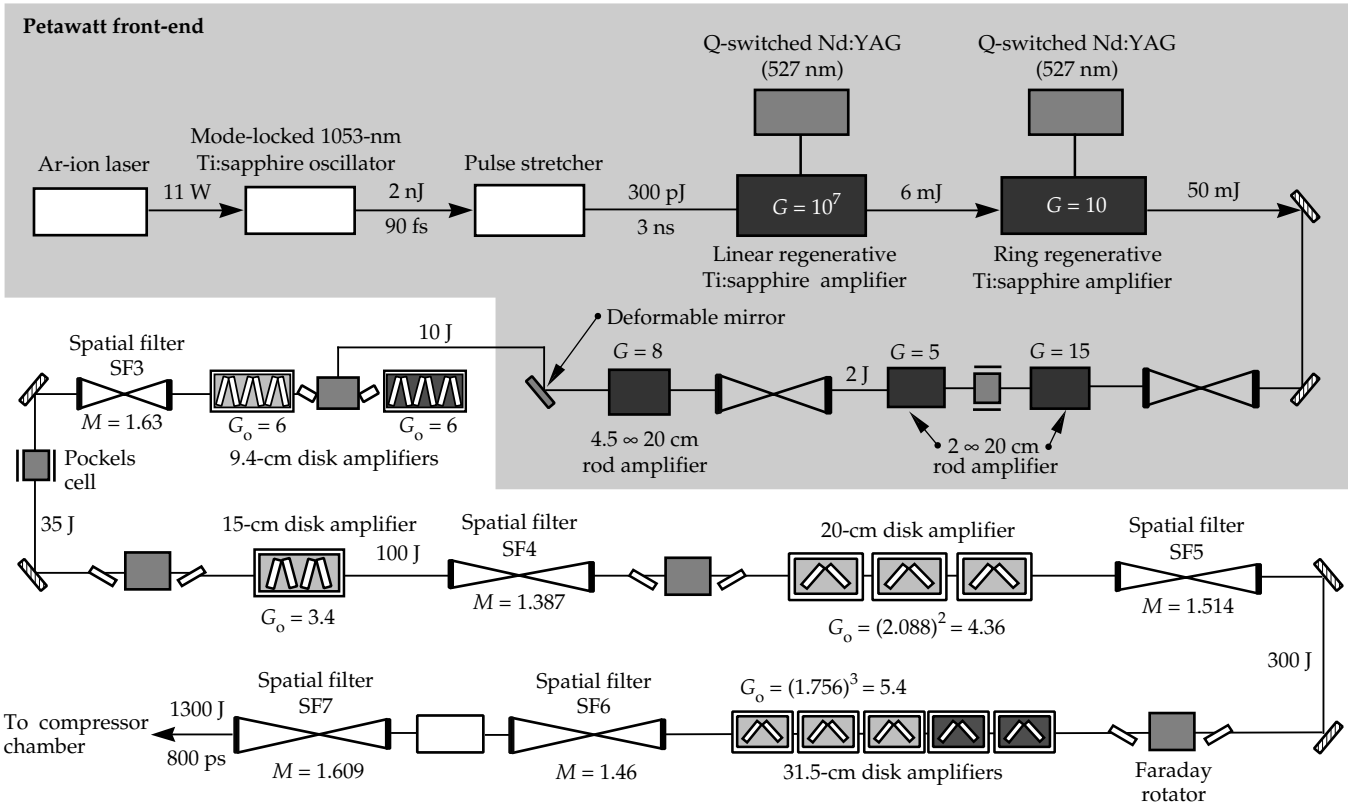

FIGURE 2. Layout of the Petawatt laser system. (70-00-0298-0180pb02)

spectral gain narrowing due both to amplification and bandwidth limiting optical components. In order to minimize the gain narrowing of the spectrum caused by high gain amplification of the laser pulse, we chose to inject the beam as far along the Nova amplifier chain as possible. Near diffraction-limited beam quality is achieved by limiting the beam to the central 80% of these amplifiers, minimizing edge effects in the disk amplifiers. A gain of only a few hundred is needed from Nova to reach the Petawatt maximum expected energy of ~1 kJ (allowing for passive transmission losses). As a result, a limited number of sets of Nova disk amplifiers provide the necessary energy, as indicated in Figure 2. The Nova 46-cm disk amplifiers are removed from the chain for Petawatt shots, as they produce a twofold problem. First, the amplifiers are split into two halves, preventing parasitic oscillations in the amplifier slab, but also destroying the coherence between the two halves of the beam. Second, the two halves of the 46-cm disks thermally distort in opposite directions when fired, steering the two halves of the beam away from each other. Together, these effects would limit the peak focal plane irradiance to much less than the diffraction limit.

Gain narrowing in the phosphate glass amplifiers reduces the spectral width to 4.0 nm and reduces the pulse duration to 800 ps. Figure 3 shows the progression of spectral gain narrowing at the output of the compressor as amplifiers were sequentially fired. The output of the two regenerative amplifiers in the Petawatt MOR is nominally Gaussian, with 65 Å bandwidth full width at half maximum (FWHM). When the two 19-mm and the 45-mm Nd:glass amplifiers in the Petawatt MOR are fired, this spectrum narrows to approximately 53 Å FWHM, producing an 18% decrease in the total bandwidth. As the beam is progressively amplified in the Nova amplifier chain, the bandwidth continues to narrow, but the spectrum remains Gaussian in shape. Addition of the 9.4-cm and 15-cm disk amplifiers reduces the spectrum by an additional 19%. In order to obtain sufficient energy out of the laser chain, all three 20-cm disk amplifiers are fired, producing another 7% reduction in bandwidth. The final three 31-cm amplifiers reduce the bandwidth by 5%. The total spectral gain narrowing observed with all amplifiers fired is ~41% from the output of the regenerative amplifiers to the output of the Nova chain.

Additional energy could be extracted from the disk amplifier section at the price of degraded spatial quality and temporal contrast upon recompression.[18] Above an intensity length product of ~100 GW/cm^2, nonlinear effects begin to degrade the beam quality, due to the intensity-dependent refractive index $n = n_0 + n_2 I$, where I is the intensity of the pulse, and n_0 and n_2 are the linear and nonlinear refractive indices, respectively.

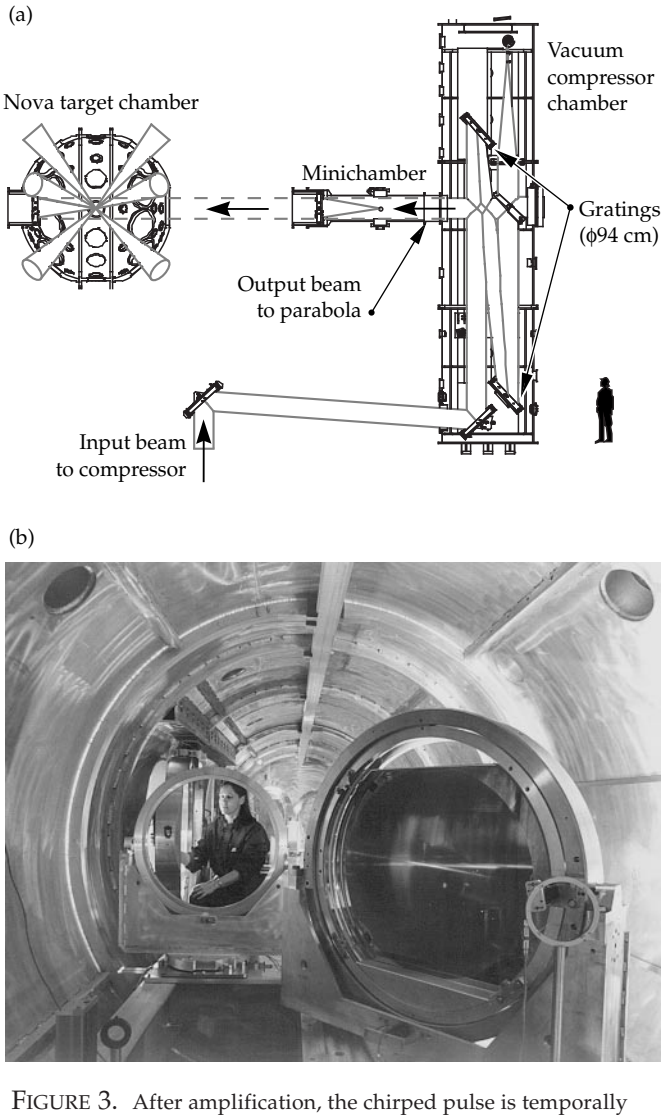

FIGURE 3. After amplification, the chirped pulse is temporally compressed in a single-pass grating compressor, then focused onto a target in an independent target chamber or integrated with Nova in the 10-beam chamber. The optical layout of the compressor is shown in (a), while a photograph of the interior of the compressor chamber (b) provides a sense of scale. (70-00-0298-0181pb03)

This intensity-dependent refractive index produces a nonlinear phase retardation that results in wavefront distortion and eventually beam filamentation.[19,20] The nonlinear phase retardation, or *B*-integral, is given by

$$B = \frac{2\pi}{\lambda}\int_0^{\ell} n_2 I(z)dz \quad ,$$

where ℓ is the propagation length.

As an example, a laser pulse propagating through 10 cm of fused silica at a power density of 10 GW/cm^2 accumulates 2 radians of nonlinear phase. The technique of CPA was developed specifically to overcome the limitations imposed by this nonlinear phase by stretching the pulse prior to amplification, thereby reducing the peak power in the amplifiers. However, economic factors dictate that petawatt-class lasers will almost always be operated at the maximum *B*-integral allowable in the laser system even with CPA. To achieve high-quality petawatt pulses on Nova, we limit the total *B*-integral to 1.0 in the Nova driver section and 1.52 in the power section, corresponding to $\Delta B \sim 2.5$ in the amplifier section.

In addition to *B*-integral, SPM in the amplifier chain can degrade the quality of the compressed pulse in CPA systems, ultimately limiting the pulse contrast.[18] This effect is easily seen by observing the increase in bandwidth of an intense, ultrashort laser pulse upon passage through a nonlinear medium according to

$$\omega(t) = \omega_0(t) - \frac{\partial B}{\partial t} \quad .$$

Spatial phase modulation is determined by the value of the nonlinear phase while frequency modulation is determined by the time-derivative. For a conventional (near transform-limited) laser pulse with the duration equal to the stretched pulse in a petawatt-class laser (500–1000 ps), the self-phase modulation effect would be negligible. However, the pulse in CPA systems is strongly chirped (i.e., exhibits a time-dependent frequency). As a result, the central part of the pulse (near the carrier frequency) experiences a greater phase retardation than the early or later part of the pulse where the intensity is less. This limits the ability to recompress the pulse and often results in temporal wings appearing on either side of the compressed pulse.[18]

Following amplification in Nova, the chirped pulse is compressed to a pulse duration which can easily be adjusted from 0.43 to 30 ps. Pulse compression occurs in a vacuum chamber with a pair of large aperture diffraction gratings arranged in a single-pass geometry, as shown in Figure 4. At the input to the compressor, the frequency components of the beam are dispersed in time from red to blue. As the beam propagates to the second grating, the blue components catch up with the red components. The second grating stops the dispersion process, producing a temporally compressed pulse. The optical throughput of the compressor was determined to be 84%. The compressed beam is reflected off a full-aperture beamsplitter to an on-axis parabolic mirror, located in a target chamber adjacent to the compressor chamber.

In small-scale CPA systems, the beam ellipticity and spatial chirp associated with a single-pass compressor geometry would be intolerable. However, in the limit that the diameter of the beam is much larger than the dispersed length, these effects are negligible. Currently, the Petawatt operates with a 46-cm beam and a dispersion length of ($c\tau_{str} \cdot \cos\theta_{compressor}$) ~20 cm. This

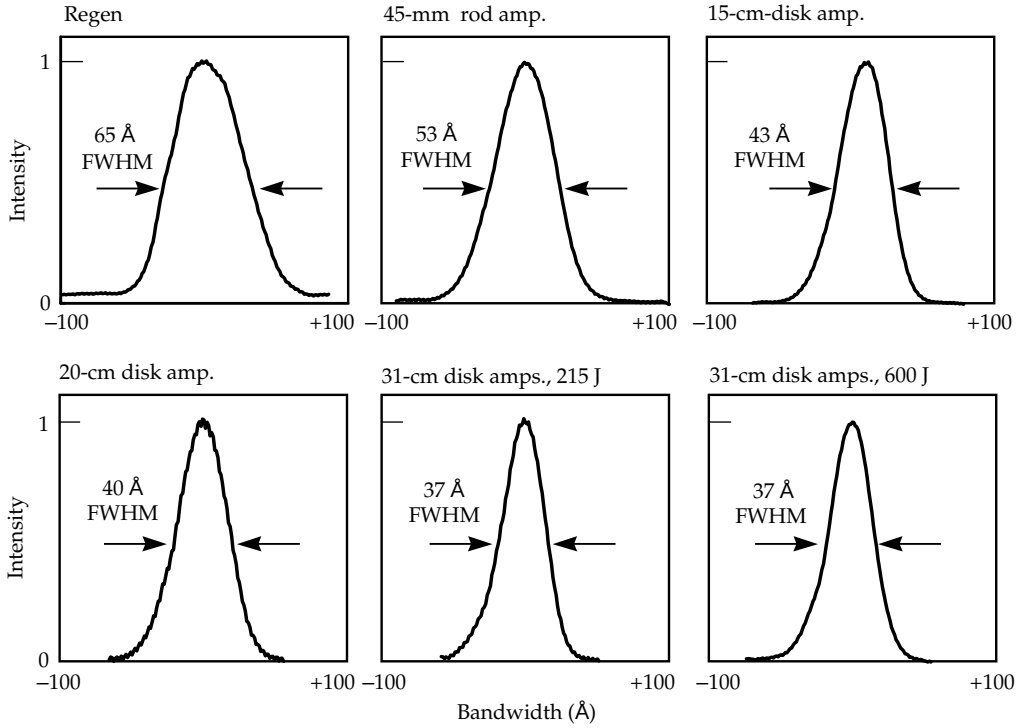

FIGURE 4. Progression of spectral gain narrowing (measured at the output of the compressor) as amplifiers were sequentially fired. (70-00-0298-0182pb01)

system is limited to a maximum pulse energy of 650 J due to the use of subaperture (74 cm) diffraction gratings. These gratings exhibit a diffraction efficiency of 95%, a diffracted wavefront quality of better than 0.1 μm (peak to valley) and a damage threshold of 0.42 J/cm^2 for 1054 nm pulses at 200 fs.[14] These gratings are currently being exchanged for full 94-cm size gratings, which will allow operation of the Petawatt at >900 J with a 58-cm-diameter beam in January 1998.

Most CPA laser systems are designed to produce the minimum pulse duration upon recompression. This is accomplished by setting the compressor to cancel the dispersion of the stretcher and optical material. Since the compressor cannot cancel the dispersion of the stretcher and optical material in the laser system exactly, the system is designed to minimize the residual phase, $\delta = \phi_{com}(\omega) + \left[\phi_{str}(\omega) + \phi_{mat}(z,\omega)\right] = 0$. These phase functions are often written in a Taylor series expansion,

$$\phi_{mat}(z,\omega) = \beta_1(\omega-\omega_0)z + \frac{\beta_2(\omega-\omega_0)^2}{2!}z + \frac{\beta_3(\omega-\omega_0)^3}{3!}z + \frac{\beta_4(\omega-\omega_0)^4}{4!}z + \ldots$$

where $\beta_n = (\partial n_k/\partial\omega^n)\omega = \omega_0$. The stretcher/compressor combination in the Petawatt laser are designed to correct for chromatic aberration and material dispersion in the system up to third-order (i.e., only the fourth-order terms in δ remain). This is sufficient for pulses of duration greater than 100 fs.

Diagnostics are located throughout the laser system to characterize and optimize its performance. Spectra, energy, pulse length measurements, and near-field irradiance are obtained in the MOR at the output of the 45-mm amplifier, in the Nova output sensor diagnostic, and at the output of the Petawatt compressor. A low-energy beam sample transmitted through the final beam splitter allows laser diagnostic measurements following compression. Parameters measured on each shot include energy, near-field irradiance, far-field irradiance, second-order autocorrelation, spectrum, and prepulse measurements. A Hartmann sensor for measuring the wavefront of the beam at low power is also located in the diagnostic station at the output of the compressor. Output pulse characteristics of the Petawatt beam under current operational conditions are shown in Figure 5. The fine-scale structure in this figure is the result of individual elements of the charge-coupled device (CCD) array used to record the data. For the Gaussian spectrum shown in Figure 5(a), the compressed pulse width is near transform limited, with a time-bandwidth product of $\Delta\nu\Delta\tau \sim 0.43$. The autocorrelation shown in Figure 5(b) indicates that on the order of a few percent of the energy is in the temporal wings of the pulse. The highest peak power achieved to date with the Petawatt laser is 1.23 PW, with 680 J out of

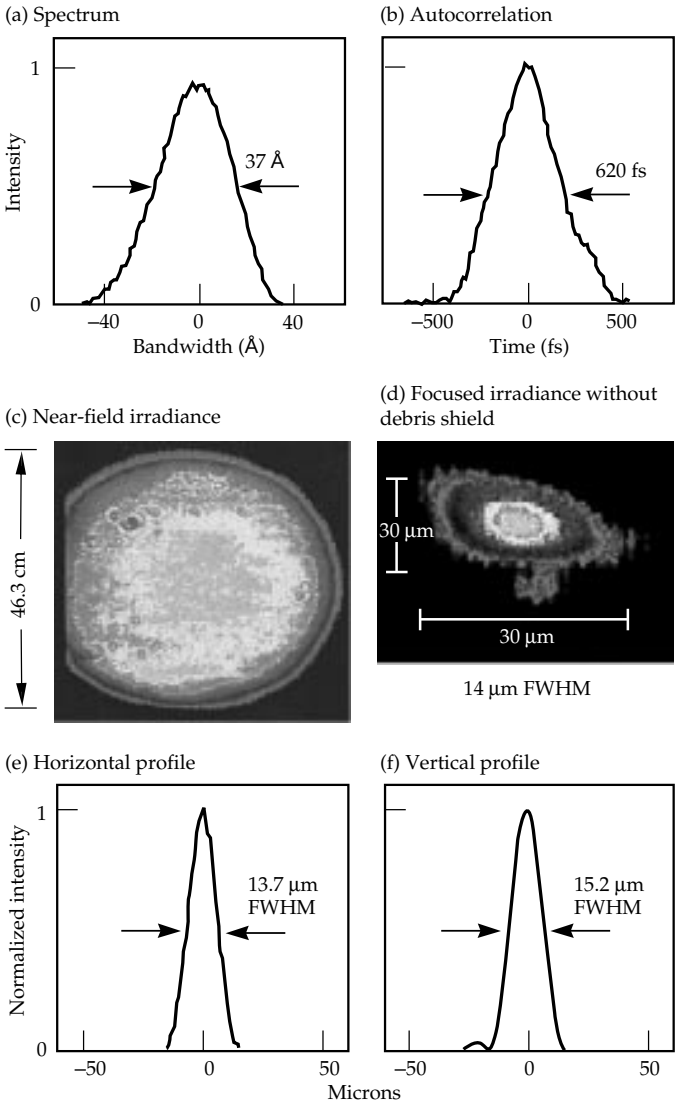

FIGURE 5. A representative sample of the Petawatt (a) spectrum, (b) autocorrelation, and (c) near-field irradiance measured on each shot in the Petawatt diagnostic station. (d) shows the focal plane distribution measured at target chamber center at 10 Hz. Intensity lineouts of this focal spot shown in (e) and (f) indicate the spot is approximately 14 µm FWHM. (70-00-0298-0183pb01)

the Nova chain and a pulse width of ~430 fs FWHM. The near-field irradiance is shown in Figure 5(c). No evidence of optical damage was observed on the gratings at this power level, or for fluences up to 400 mJ/cm^2.

Targeting System and Experiments

Target experiments with petawatt pulses will be possible either in an independent target chamber or with the Nova laser system for integrated fast ignition experiments. A one-beam chamber has been installed in between the Petawatt compressor and the 10-beam chamber to allow single-beam experiments. The primary target chamber focusing optic is an on-axis parabolic mirror, nominally $f/3$. The entire parabola assembly is transferable between the one-beam and 10-beam chambers for integrated experiments with the Petawatt beam and Nova at some point in the future.

A microscope and reticle assembly are used to measure the focal spot size at the target chamber center. A representative image of the focal spot measured at the target chamber center at 10 Hz is shown in Figure 5(d). We have measured a primary focus directly off the parabolic mirror as small as 14 µm FWHM [Figure 5(e)]. Change in the stresses applied by the grating mounts has caused a gradual degradation of grating wavefront over time, resulting in a current focal spot on the order of 26 × 38 µm FWHM. These wavefront distortions will be corrected with the implementation of the deformable mirror. Thermal distortion of the amplifier disks due to repeated firing throughout the day causes the focal distribution to broaden by a factor of 2 to 3, as expected. These pump-induced aberrations can also be compensated with the use of the deformable mirror wavefront correction system, which will be operational in early 1998. Experiments on the Beamlet laser have shown that deformable mirror pre-correction can produce a nearly diffraction-limited focal spot.[21] With the deformable mirror system, the Petawatt laser system should achieve a near diffraction-limited focal spot with a high shot rate.

For long-pulse (5–20 ps) fast ignitor physics experiments, the parabola is protected from target debris by a full-aperture debris shield. For short-pulse experiments, however, a conventional 1-cm-thick fused silica debris shield would produce an unacceptable accumulation of nonlinear phase retardation, ~28 radians double-passed! To protect the parabola from line-of-sight debris without incurring a large nonlinear phase retardation, a secondary "plasma mirror" is used in conjunction with the primary parabola, as shown in Figure 6.[22] For irradiances > 2×10^{14} W/cm^2, short-pulse radiation creates a critical-density plasma on the surface of a dielectric substrate. For incident pulses on the order of 500 fs, the plasma has insufficient time to undergo hydrodynamic expansion, producing a density-scale length less than the incident wavelength. This produces a reflecting plasma with a reflected wavefront comparable in quality to that of the initial surface. Reflectivities exceeding 90% have been achieved. Small-scale measurements made with the Petawatt front-end are in good agreement with the theoretical calculations shown in Figure 7. This novel targeting system enables the production of high-contrast

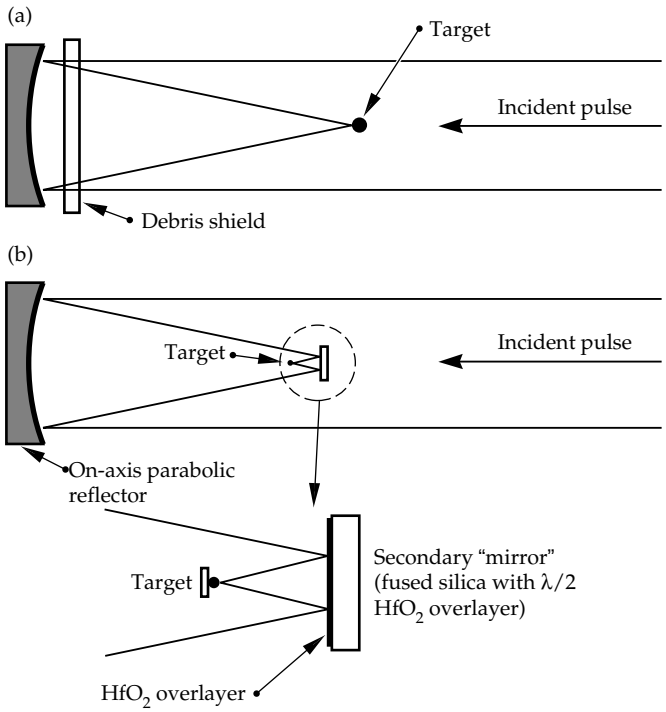

FIGURE 6. (a) A conventional debris shield cannot be used in the Petawatt targeting system for short pulses. The accumulated nonlinear phase retardation for double-pass through a 1-cm-thick fused silica debris shield would produce 28 radians of *B*. (b) Line-of-sight debris can be eliminated by focusing with a spherical plasma mirror in conjunction with an incident target shield. (70-00-0298-0184-pb01)

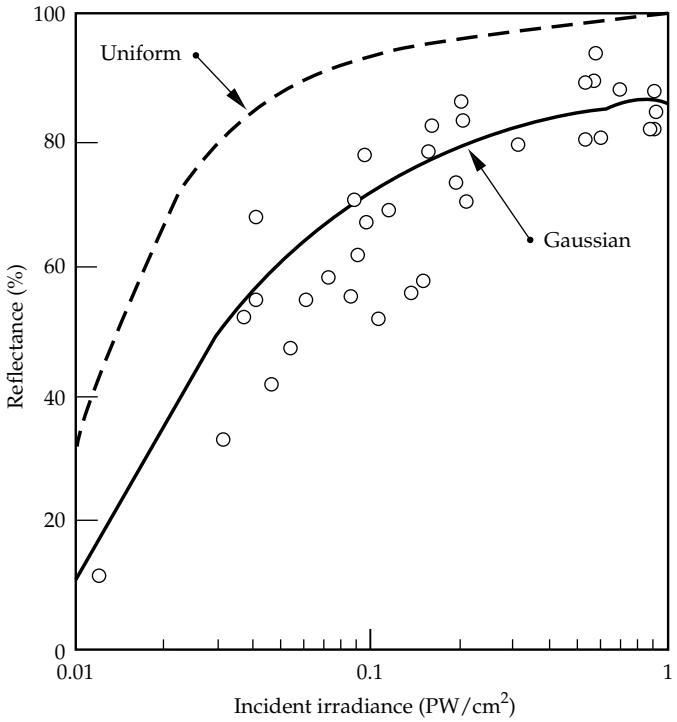

FIGURE 7. Small-scale experiments done at the output of the Petawatt front-end indicate that greater than 90% reflectivity can be achieved with good reflected wavefront quality. Measurements are in good agreement with the theoretical calculations. (70-00-0298-0185pb01)

pulses (10^7), when an antireflection-coated substrate is used. In addition, by using a curved plasma mirror, the effective focal length of the system can be easily varied. Initial experiments with the plasma mirror on gold targets showed molten gold from the target hit the mirror surface, and splattered back onto the parabolic mirror. Future experiments will prevent this by placing the target inside a large disk to protect the parabola from line-of-sight debris, or by using an off-axis geometry. Currently all experiments with the Petawatt are performed in the one-beam chamber.

Two classes of experiments have been performed to date using the Petawatt laser. Long-pulse (~20 ps) experiments address fast ignitor physics, while initial short-pulse (~500 fs) experiments were designed to demonstrate the potential use of the Petawatt as a source for laser-driven radiography. Figure 8 shows a photographic image of a long-pulse beam target experiment with the Petawatt laser. The laser pulse is entering from left. The background green light is the result of second harmonic emission from the target. Particles emerging from the back of the target can be observed in a series of jets at right. K-α fluorescence induced in a molybdenum layer buried in a solid aluminum target provides a measure of the conversion efficiency of laser light to electrons. Up to 35% conversion to electrons of mean energy 1 MeV at 2×10^{19} W/cm^2 has been measured.[23]

Recent short-pulse experiments delivered up to 330 J on target with pulse length 420–500 fs, for a peak irradiance of 1.7×10^{20} W/cm^2. These experiments examined the creation of hot (0.1–1 MeV) electrons by high-irradiance pulses. By changing the

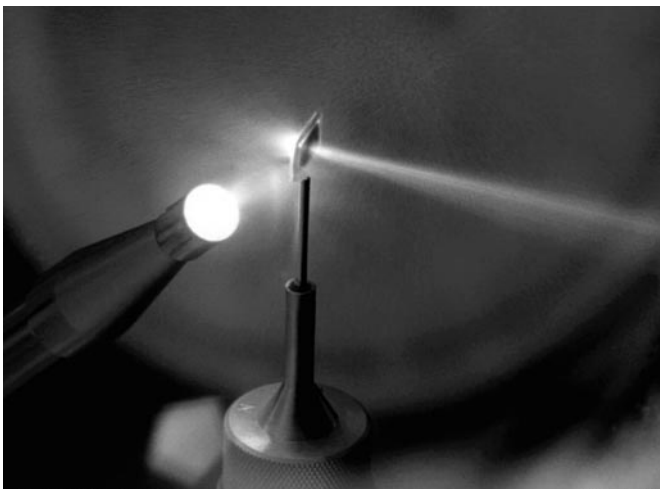

FIGURE 8. Photographic image of single-beam target experiment with the Petawatt laser taken by G. Stone. The laser pulse is entering from left. The background light is green resulting from second harmonic emission from the target. Particles emerging from the back of the target can be observed in a series of jets at right. (70-60-0597-0766.4pb01)

experimental conditions, the electron spectrum can be shifted towards higher energy (10–100 MeV), even in solid-density plasmas. High-field magnetic dipole spectrometers were fielded at 30° and 95° off the laser axis to measure the electron spectrum (from 0.1 to 150 MeV) emerging from the back of the target and orthogonal to the laser axis. The dispersed electron spectrum is recorded as tracks in a standard emulsion. A representative electron spectrum produced from a 0.5-mm-thick gold target shot at near normal incidence is shown in Figure 9. Electrons were observed at energies extending above 90 MeV; however, the bulk of the distribution was in the range of ~5 to 15 MeV, where the emission was found to be forward directed with about ten times more flux observed at 30°, with respect to the laser propagation direction, as compared to the flux at 95°.

High-energy bremsstrahlung x rays generated by the electrons in the gold target produced photonuclear reactions in both the gold and surrounding copper target-holder. These reactions produced activation and transmutation to platinum and nickel daughter isotopes. Some specific reactions observed include ^{197}Au(γ,n)^{196}Au, identified by the decay of the ^{196}Au to ^{196}Pt emitting nuclear gamma rays at 356 and 333 keV, and ^{63}Cu(γ,n)^{62}Cu and ^{65}Cu(γ,n)^{64}Cu, which were identified by their subsequent beta decay to ^{62}Ni and ^{64}Ni with half-lives of 9.7 minutes and 12.7 hours, respectively. The threshold gamma-ray energy for photo-activation of the gold and copper is ~8 and ~11 MeV, respectively, indicating a large flux of high-energy bremsstrahlung. A gamma spectrum and decay curve are shown in Figure 10. Neutron spectra and other high-energy x-ray spectra are also routinely measured. Together, these diagnostics are providing us the first glimpse into this new regime of laser–matter interactions.

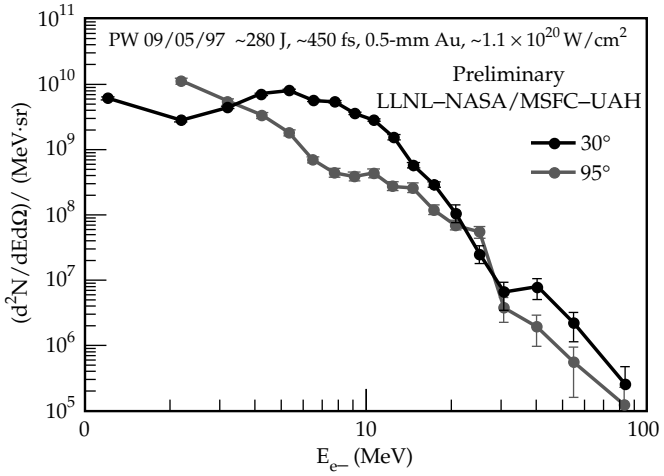

FIGURE 9. Electron spectrum produced in 0.5-mm gold target at 1.1×10^{20} W/cm^2. (70-00-0298-0187pb01)

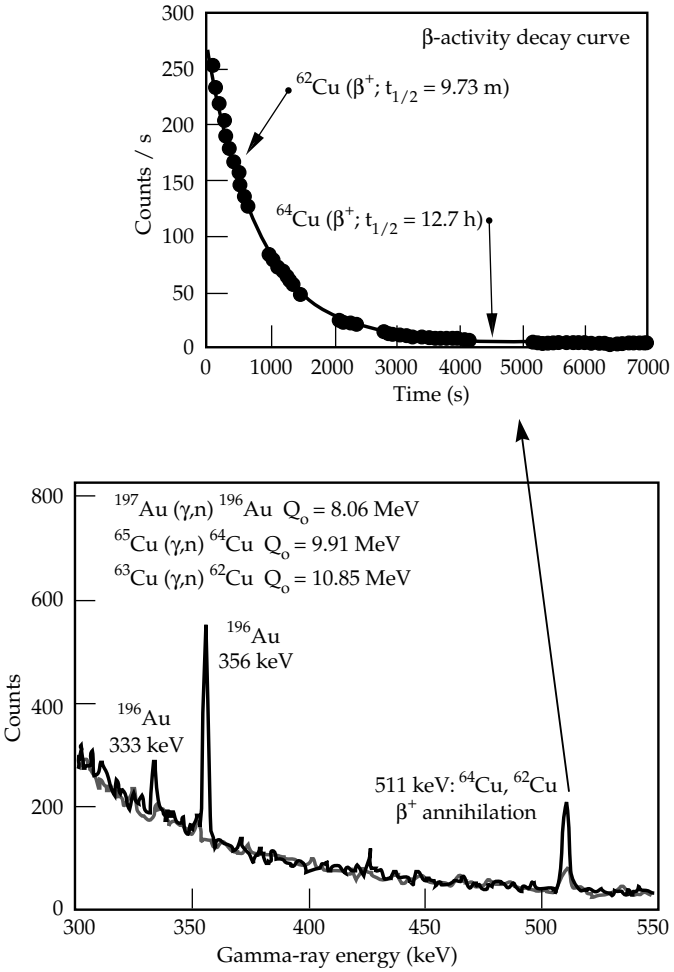

FIGURE 10. Photonuclear activation spectrum taken on a short-pulse Petawatt target. (70-00-0298-0188pb01)

Summary

The overall performance of the Petawatt laser to date has exceeded expectations. We have demonstrated the production of 1.23 petawatt of peak power in the Nova/Petawatt Laser Facility, generating >600 J in <500 fs. Currently, this system is limited to 600-J pulses in a 46.3-cm beam. Expansion of the beam to 58 cm, with the installation of 94-cm gratings, will enable >900-J operation. Focusing the beam onto a target is accomplished using an on-axis parabolic mirror with a debris shield for 5- to 20-ps pulse length, or in conjunction with a plasma mirror for pulse lengths <5 ps. Recent short-pulse experiments (with pulse length 420–500 fs) delivered up to 330 J on target, for a world-record peak irradiance of 1.7×10^{20} W/cm^2. With the installation of the full-aperture gratings and deformable mirror, an irradiance of 10^{21} W/cm^2 should be achievable. Target experiments with petawatt pulses have concentrated on the demonstration of fast ignitor physics and the potential use of the petawatt-class lasers as a source for laser-driven radiography.

Acknowledgments

In a project the size and scale of the Petawatt Laser System, the success was enabled by the contributions of many people, in particular the staff of Nova Engineering and Operations. Significant contributions were made to the gratings development effort by B. Shore, B. Boyd, and H. Nguyen. Target experiments were performed in collaboration with T. Cowan, S. Hatchett, A. Hunt, M. Key, J. Koch, J. Moody, M. Moran, T. Phillips, C. Sangster, R. Snavely, M. Tabak, K. Wharton, S. Wilks, and others. Analysis of the electron spectrometer film emulsions was performed by W. Fountain, J. Johnson, T. Parnell, and Y. Takahashi of the University of Alabama and NASA Marshall Space Flight Center.

References

1. M. D. Perry and G. Mourou, *Science*, **264**, 917–924 (1994).
2. C. Joshi and P. B. Corkum, *Physics Today* (1996).
3. M. Tabak, J. Hammer, M. E. Glinsky, W. L. Kruer, S. C. Wilks, J. Woodworth, E. M. Campbell, M. D. Perry, and R. J. Mason, *Phys. Plasmas*, **1**, 1626–1634 (1994).
4. J. Lindl, *Phys. Plasmas*, **2**, 3933–4024 (1995).
5. C. E. Cook, *Proc. IRE*, **48**, 310–316 (1960).
6. R. A. Fisher and W. K. Bischel, *IEEE J. Quantum Electron.*, **QE-11**, 46–52 (1975).
7. D. Strickland and G. Mourou, *Opt. Comm.*, **56**, 219–221 (1985).
8. C. Sauteret, D. Husson, G. Thiell, S. Seznac, et al., *Opt. Lett.*, **16**, 238 (1991).
9. C. Rouyer, E. Mazataud, I. Allais, A. Pierre, S. Seznac, C. Sauteret, and G. Mourou, *Opt. Lett.*, **18**, 214–216 (1993).
10. C. N. Danson, L. Barzanti, Z. Chang, A. Damerell, et al., *Opt. Comm.*, **103**, 392–397 (1993).
11. K. Yamakawa, H. Shiraga, and Y. Kato, *Opt. Lett.*, **16**, 1593 (1991).
12. M. D. Perry, F. G. Patterson, and J. Weston, *Opt. Lett.*, **15**, 381–383 (1990).
13. B. C. Stuart, M. D. Perry, J. Miller, G. Tietbohl, S. Herman, J. A. Britten, C. Brown, D. Pennington, and V. Yanovsky, *Opt. Lett.* (1997).
14. R. Boyd, J. Britten, D. Decker, B. W. Shore, B. C. Stuart, M. D. Perry, and L. Li, *Appl. Opt.*, **34**, 1697–1706 (1995).
15. B. C. Stuart, S. Herman, and M. D. Perry, *IEEE J. Quantum Electron.*, **31**, 528–538 (1995).
16. B. C. Stuart, M. D. Feit, A. M. Rubenchik, B. W. Shore, and M. D. Perry, *Phys. Rev. Lett.*, **74**, 2248–2251 (1995).
17. B. C. Stuart, M. D. Feit, A. M. Rubenchik, B. W. Shore, and M. D. Perry, *Phys. Rev. B*, **53**, 1749–1761 (1996).
18. M. D. Perry, T. Ditmire, and B. C. Stuart, *Opt. Lett.*, **19**, 2149–2151 (1994).
19. Y. R. Shen, *The Principles of Nonlinear Optics* (Wiley, New York, NY, 1984).
20. W. Koechner, *Solid-State Laser Engineering*, 3rd ed. (Springer–Verlag, New York, NY, 1990).
21. B. M. V. Wonterghem, E. S. Bliss, J. A. Caird, R. G. Hartley, M. W. Kartz, J. T. Salmon, and P. J. Wegner, paper presented at Solid-State Lasers for Application to Inertial Confinement Fusion, Paris, France, 1996.
22. M. D. Perry, V. Yanovsky, M. Feit, and A. Rubenchik, *Phys. Plasmas*, to be submitted, 1997.
23. K. Wharton, *Phys. Rev. Lett.*, to be submitted, 1997.